Inorg. Chem. **2004**, *43*, 4767–4774

Inorganic Chemistry
Article

# Novel One-Dimensional Polymers Generated from *p*-Ferrocenylbenzoate: Syntheses, Structures, and Magnetic Properties

**Hongwei Hou,* Linke Li, Yu Zhu, Yaoting Fan, and Yuqin Qiao**

*Department of Chemistry, Zhengzhou University, Henan 450052, P. R. China*

Received March 3, 2004

Treatment of *p*-ferrocenylbenzoate [*p*-$HOOCH_4C_6Fc$, Fc = $(\eta^5\text{-}C_5H_5)Fe(\eta^5\text{-}C_5H_5)$] with $Mn(OAc)_2{\cdot}2H_2O$ or $Cd(OAc)_2{\cdot}2H_2O$ afforded one-dimensional linear chain polymer $\{[Mn(OOCH_4C_6Fc)_2(\mu_2\text{-}OH_2)(H_2O)_2](H_2O)\}_n$ (**1**), double-bridge polymer $[Mn(\mu_2\text{-}OOCH_4C_6Fc)_2(phen)]_n$ (phen = phenanthroline) (**2**), and ladderlike framework $\{[Cd(\mu_2\text{-}OOCH_4C_6Fc)(\eta^2\text{-}OOCH_4C_6Fc)(bbp)](CH_3OH)\}_n$ (bbp = 4,4′-trimethylene-dipyridine) (**3**). The solution-state cyclic voltammograms indicate that the half-wave potentials of the ferrocenyl moieties in these polymers are all shifted to positive potential compared to that of sodium *p*-ferrocenylbenzoate. Both **1** and **2** behave as 1D Heisenberg Mn(II) chains with weak intrachain antiferromagnetic interactions between the local high-spin Mn(II) ions, and the exchange coupling parameters $J$ (–5.20 and –3.25 $cm^{-1}$ for **1** and **2**, respectively) are larger than those of most of the reported di-Mn(II) complexes that contain $\mu_2$-aqua and $\mu_2$-carboxylato units and one-dimensional Mn(II) carboxylic polymers.

## Introduction

Currently, researchers are showing much interest in the solid-state chemistry of molecularly derived solids with extended linkages.[1,2] An intelligent choice of building block might yield materials with fascinating structures and desirable properties. Also in recent years, a number of excellent bridging ligands have been explored to link metal ions together to form novel topologies that might exhibit interesting properties as potential new materials.[3] Among such materials, carboxylate ligands are one kind of excellent building blocks for bridging metal centers, and they are tactic candidates for the formation of extended arrays.[4,5]

The ferrocene carboxylate-containing compounds were synthesized some years ago, but their coordination properties have not been intensively explored.[6] In fact, as a ligand, ferrocene carboxylate-containing compounds have many advantages: The versatile coordination capacity of the carboxylate group makes the self-assembly of crystal engineering easily available. Furthermore, the incorporation of the ferrocene moiety into the metal–organic framework can combine the organometallic with polymeric properties and provide an effective method of preparing new functional materials with unique features in addition to the merits of organometallic and coordination polymers that might be suitable for use in the electrical, magnetic, preceramic, catalytic, and nonlinear optics (NLO) fields.[7] On these bases, introducing bulky ferrocene carboxylate-containing groups into polymeric chemistry and further exploiting the relationship between the structures and properties of these groups

---

* To whom correspondence should be addressed. E-mail: houhongw@zzu.edu.cn. Tel. and Fax: +86-371-7761744.

(1) (a) Smart, L.; Moore, E. *Solid State Chemistry*; Chapman and Hall: London, 1992. (b) Cheetham, A. K., Day, P., Eds. *Solid State Chemistry*; Clarendon Press: Oxford, U.K., 1992.

(2) (a) Thomas, J. M. *Angew. Chem.* **1998**, *27*, 1673. (b) Suib, S. L. *Chem. Rev.* **1993**, *93*, 803. (c) Disalvo, F. J. *Science* **1990**, *247*, 649.

(3) (a) Horikoshi, R.; Mochida, T.; Moriyama, H. *Inorg. Chem.* **2001**, *40*, 2430. (b) Horikoshi, R.; Nambu, C.; Mochida, T. *Inorg. Chem.* **2003**, *42*, 6868. (c) Gao, E. Q.; Bai, S. Q.; Wang, Z. M.; Yan, C. H. *J. Chem. Soc., Dalton Trans.* **2003**, 1759. (d) Losier, P.; Zaworotko, M. J. *Angew. Chem., Int. Ed. Engl.* **1996**, *35*, 2779. (e) Blake, A. J.; Champness, N. R.; Chung, S. S. M.; Li, W.; Schröder, M. *Chem. Commun.* **1997**, 1005. (f) Jung, O. S.; Park, S. O.; Kim, K. M.; Jang, H. G. *Inorg. Chem.* **1998**, *37*, 5781. (g) Bu, X. H.; Tong, M. L.; Chang, H. C.; Kitagawa, S.; Batten, S. R. *Angew. Chem., Int. Ed.* **2004**, *43*, 192. (h) Carlucci, L.; Ciani, G.; Proserpio, D. M.; Porta, F. *Angew. Chem., Int. Ed.* **2003**, *42*, 317.

(4) (a) Cannon, R. D.; White, R. P. *Prog. Inorg. Chem.* **1988**, *36*, 195. (b) Cotton, F. A.; Duraj, S. A.; Roth, W. J. *Inorg. Chem.* **1984**, *23*, 4042. (c) Cotton, F. A.; Lewis, G. E.; Mott, G. N. *Inorg. Chem.* **1983**, *22*, 1825. (d) Koh, Y. B.; Christoph, G. G. *Inorg. Chem.* **1979**, *18*, 1122. (e) Rueff, J. M.; Masciocchi, N.; Rabu, P.; Sironi, A.; Skoulios, A. *Eur. J. Inorg. Chem.* **2001**, 2843.

(5) (a) Dai, J. C.; Wu, X. T.; Fu, Z. Y.; Hu, S. M.; Du, W. X.; Cui, C. P.; Wu, L. M.; Zhang, H. H.; Sun, R. Q. *Chem. Commun.* **2002**, 12. (b) Yaghi, O. M.; Davis, C. E.; Li, G. M.; Li, H. L. *J. Am. Chem. Soc.* **1997**, *119*, 2861. (c) Li, Y. G.; Hao, N.; Lu, Y.; Wang, E. B.; Kang, Z. H.; Hu, C. G. *Inorg. Chem.* **2003**, *42*, 3119. (d) Tao, J.; Tong, M. L.; Chen, X. M. *J. Chem. Soc., Dalton Trans.* **2000**, 3669. (e) Hong, C. S.; Do, Y. *Inorg. Chem.* **1998**, *37*, 4470. (f) Cao, R.; Sun, D.; Liang, U.; Hong, M.; Tatsumi, K.; Shi, Q. *Inorg. Chem.* **2002**, *41*, 2087.

10.1021/ic049728x CCC: $27.50

has constituted one of the most attractive research fields in modern structural chemistry.

Some groups including ours have utilized a series of ferrocene carboxylate-containing ligands to react with metal ions and produced some novel and interesting topological complexes,[6] such as the one-dimensional polymeric complexes $\{[Pb(\mu_2\text{-}\eta^2\text{-OOCCH}{=}(CH_3)CFc)_2]\cdot MeOH\}_n$,[6b] $\{[Cd(o\text{-OOCC}_6H_4COFc)_2(bpe)(MeOH)\cdot 2H_2O]_n$ (bpe = 1,2-bis(4-pyridyl)ethane),[6b] $\{[Zn(FcCOO)_2(bpt)\cdot 2.5H_2O]_n$ (bpt = *N*,*N*′-bis(3-pyridylmethyl)thiourea),[6d] and tin−oxygen cluster $[\{BuSn(O)OC(O)Fc\}_6]$.[8] However, most of the reported ferrocene carboxylate-containing polymeric complexes have $d^{10}$ metal centers (Zn, Pb, Cd, Sn, etc.).

As a part of our work toward the rational design and preparation of functional coordination frameworks and in an effort to further study $d^{<10}$ and $d^{10}$ metal ferrocene carboxylate-containing polymeric complexes, we used sodium *p*-ferrocenylbenzoate to react with Mn(II) and Cd(II) and obtained three novel one-dimensional polymers: $\{[Mn(OOCH_4C_6Fc)_2(\mu_2\text{-}OH_2)(H_2O)_2](H_2O)\}_n$ (**1**), $[Mn(\mu_2\text{-OOCH}_4C_6Fc)_2(phen)]_n$ (phen = phenanthroline) (**2**), and $\{[Cd(\mu_2\text{-OOCH}_4C_6Fc)(\eta^2\text{-OOCH}_4C_6Fc)(bbp)](CH_3OH)\}_n$ (bbp = 4,4′-trimethylene-dipyridine) (**3**). To our knowledge, no such polymers containing Mn(II) ions have been reported up to now. Herein, we report the syntheses, structural characterizations, thermal stabilities, and electrochemical properties of these polymers and further make a detailed description of the magnetic properties of polymers **1** and **2**.

## Experimental Section

**General Details.** All chemicals were of reagent-grade quality and were obtained from commercial sources and used without further purification. *p*-Ferrocenylbenzoic acid and its sodium salt was prepared according to a literature method.[9]

**Preparation of $\{[Mn(OOCH_4C_6Fc)_2(\mu_2\text{-}OH_2)(H_2O)_2](H_2O)\}_n$ (1).** The reaction of $Mn(OAc)_2\cdot 2H_2O$ (26.8 mg, 0.1 mmol) with 0.2 mmol (65.6 mg) of $FcC_6H_4COONa$ in a mixture solution of $H_2O$ (3 mL) and methanol (6 mL) resulted in crystals of **1**. The resultant orange solution was allowed to stand at room temperature in the dark. Light yellow crystals suitable for X-ray diffraction were obtained 2 weeks later. Yield: 68%. Anal. Calcd for $C_{34}H_{36}O_8Fe_2Mn$: C, 55.24; H, 4.91. Found: C, 55.19; H, 4.96. IR ($cm^{-1}$, KBr): 3422 (s), 3091 (m), 1604 (s), 1534 (s), 1403 (s), 1180 (m), 1105 (m), 1006 (m), 819 (m), 789 (m), 708 (m), 476 (m).

**Preparation of $[Mn(\mu_2\text{-OOCH}_4C_6Fc)_2(phen)]_n$ (2).** Four milliliters of a methanol solution of phen (19.8 mg, 0.1 mmol) (phen = phenanthroline) was added to an aqueous solution (2 mL) of $Mn(OAc)_2\cdot 2H_2O$ (26.8 mg, 0.1 mmol), and then 5 mL of methanol solution of $FcC_6H_4COONa$ (65.6 mg, 0.2 mmol) was added dropwise to the above mixture. The resultant orange solution was allowed to stand at room temperature in the dark. After 1 week, good-quality red crystals of **2** were obtained. Yield: 58%. Anal. Calcd for $C_{46}H_{34}Fe_2O_4N_2Mn$: C, 65.35; H, 4.05; N, 3.31. Found: C, 65.32; H, 4.09; N, 3.26. IR ($cm^{-1}$, KBr): 3426 (s), 3100 (m), 1643 (s), 1595 (s), 1548 (s), 1395 (s), 1102 (m), 790 (m), 726 (m), 472 (m).

**Preparation of $\{[Cd(\mu_2\text{-OOCH}_4C_6Fc)(\eta^2\text{-OOCH}_4C_6Fc)(bbp)](CH_3OH)\}_n$ (3).** A methanol solution (4 mL) of bbp (1.98 mg, 0.1 mmol) (bbp = 4,4′-trimethylene-dipyridine) was added dropwise to 4 mL of an aqueous solution of $Cd(OAc)_2\cdot 2H_2O$ (26.8 mg, 0.1 mmol), giving a clear solution. $FcC_6H_4COONa$ (65.6 mg, 0.2 mmol) in 6 mL of methanol was added dropwise to the above mixture solution. Two weeks later, crystals suitable for X-ray diffraction were obtained from the resultant orange solution that had been left standing at room temperature in the dark. Yield: 63%. Anal. Calcd for $C_{48}H_{44}O_5N_2Fe_2Cd$: C, 60.50; H, 4.65; N, 2.94. Found: C, 60.58; H, 4.69; N, 2.89. IR ($cm^{-1}$, KBr): 3426 (s), 3112 (m), 1604 (s), 1535 (s), 1396 (s), 1012 (m), 795 (m), 709 (m), 475 (m).

**Physical Measurements.** C, H, and N analyses were carried out on a Carlo-Erba 1106 elemental analyzer. IR data were recorded on a Bruker TENSOR 27 spectrophotometer with KBr pellets in the 400−4000 $cm^{-1}$ region.

The molecular weights and molecular weight distributions of the polymers were determined at 40 °C with gel permeation chromatography (Waters Associates model HPLC/GPC 515 liquid chromatograph, equipped with a refractive index detector and $\mu$-Styragel columns and calibrated with standard polystyrene), using DMF as the eluent and a flow rate of 1.0 $mLmin^{-1}$.

Powder X-ray diffraction (PXRD) data were recorded on a Rigaku D/MAX-3B diffractometer for Cu K$\alpha$ radiation, with a step size of 0.2° in $\theta$ and a scan speed of 6° per step.

TGA−DTA measurements were obtained by heating the sample from 20 to 900 °C at a rate of 10 °C $min^{-1}$ in air on a Perkin-Elmer DTA-7 and TGA-7 differential thermal analyzer. (See Supporting Information.)

Cyclic voltammograms were recorded with a CHI650 electrochemical analyzer utilizing the three-electrode configuration of a Pt working electrode, a Pt auxiliary electrode, and a commercially available saturated calomel electrode as the reference electrode with a pure $N_2$ gas inlet and outlet. The measurements were made in DMF solution containing tetraethylammonium perchlorate ($n\text{-}Bu_4NClO_4$) (0.1 $mol\cdot dm^{-3}$) as the supporting electrolyte, which has a 50-ms pulse width and a 20-ms sample width. The potential was scanned from +0.2 to +0.9 V at scan rate of 100 mV $s^{-1}$. (See Supporting Information.)

Temperature-dependent magnetic susceptibility measurements on powdered solid samples were made on a SQUID magnetometer (MPMS Quantum Design) over the temperature range 300−5 K. The magnetic field applied was 500 G. The observed susceptibility

---

(6) (a) Prokopuk, N.; Shriver, D. F. *Inorg. Chem.* **1997**, *36*, 5609. (b) Li, G.; Hou, H. W.; Li, L. K.; Meng, X. R.; Fan, Y. T.; Zhu, Y. *Inorg. Chem.* **2003**, *42*, 4995. (c) Hou, H. W.; Li, G.; Li, L. K.; Zhu, Y.; Fan, Y. T. *Inorg. Chem.* **2003**, *42*, 428. (d) Hou, H. W.; Li, L. K.; Li, G.; Fan, Y. T.; Zhu, Y. *Inorg. Chem.* **2003**, *42*, 3501. (e) Guo, D.; Mo, H.; Duan, C. Y.; Lu, F.; Meng, Q. J. *J. Chem. Soc., Dalton Trans.* **2002**, 2593. (f) Guo, D.; Zhang, B. G.; Duan, C. Y.; Cao, X.; Meng, Q. J. *J. Chem. Soc., Dalton Trans.* **2003**, 282. (g) Meng, X. R.; Li, G.; Hou, H. W.; Han, H. Y.; Fan, Y. T.; Zhu, Y.; Du, C. X. *J. Organomet. Chem.* **2003**, *679*, 153.

(7) (a) Wisian-Neilson, P., Allcock, H. R., Wynne, K. J., EdS. *Inorganic and Organometallic Polymers II. Advanced Materials and Intermediates*; ACS Symposium Series 572; American Chemical Society: Washington, DC, 1994. (b) Sheats, J. E., Carraher, C. E., Jr., Pittman, C. U., Jr., Zeldin, M., Currell, B., Eds. *Inorganic and Metal-Containing Polymeric Materials*; Plenum Press: New York, 1990. (c) Mark, J. E., Allcock, H. R., West, R., Eds. *Inorganic Polymers*; Prentice-Hall: Englewood Cliffs, NJ, 1992. (d) Zeldin, M., Wynne, K. J., Allcock, H. R., Eds. *Inorganic and Organometallic Polymers*; ACS Symposium Series 360; American Chemical Society: Washington, DC, 1988. (e) Sheats, J. E., Carraher, C. E., Jr., Pittman, C. U., Jr., Eds. *Metal-Containing Polymeric Systems*; Plenum Press: New York, 1985. (f) Manners, I. *Angew. Chem., Int. Ed. Engl.* **1996**, *35*, 1602.

(8) Chandrasekhar, V.; Nagendran, S.; Bansal, S.; Kozee, M. A.; Powell, D. R. *Angew. Chem., Int. Ed.* **2000**, *39*, 1833.

(9) Hu, P.; Zhao, K. Q.; Zhang, L. F. *J. Si Chuan Normal. Univ. (Nat. Sci. Ed.)* **1998**, *21* (4), 433 (in Chinese).

**Table 1.** Crystallographic Data for **1−3**

| | **1** | **2** | **3** |
|---|---|---|---|
| formula | $C_{34}H_{36}Fe_2MnO_8$ | $C_{46}H_{34}Fe_2MnN_2O_4$ | $C_{48}H_{44}CdFe_2N_2O_5$ |
| fw | 739.27 | 845.39 | 952.95 |
| crystal system | monoclinic | monoclinic | triclinic |
| crystal size (mm) | 0.20 × 0.18 × 0.18 | 0.20 × 0.18 × 0.18 | 0.20 × 0.18 × 0.18 |
| space group | *C*2/*c* | *P*2(1)*c* | $P\bar{1}$ |
| *a* (Å) | 45.559(9) | 20.889(4) | 9.0012(18) |
| *b* (Å) | 9.872(2) | 21.666(4) | 12.354(3) |
| *c* (Å) | 8.1709(13) | 8.2232(16) | 19.981(4) |
| α (deg) | 90 | 90 | 93.79(3) |
| *β* (deg) | 93.03(3) | 95.16(3) | 96.53(3) |
| *γ* (deg) | 90 | 90 | 106.03(3) |
| $V$ (Å$^3$) | 3669.9(13) | 3706.6(13) | 2110.6(7) |
| $D_c$ (Mg m$^{-3}$) | 1.338 | 1.515 | 1.499 |
| *Z* | 4 | 4 | 2 |
| $\mu$ (mm$^{-1}$) | 1.163 | 1.157 | 1.226 |
| reflns collected/unique | 5136/2959 | 9624/5479 | 6908/6908 |
| *R*(int) | 0.0731 | 0.0281 | 0.0000 |
| data/restraints/parameters | 2959/0/215 | 5479/0/497 | 6908/1/527 |
| index ranges | $-53 \le h \le 53$,<br>$-11 \le k \le 0$,<br>$-9 \le l \le 9$ | $-24 \le h \le 24$,<br>$-24 \le k \le 24$,<br>$0 \le l \le 9$ | $-11 \le h \le 11$,<br>$0 \le k \le 15$,<br>$-25 \le l \le 25$ |
| *F*(000) | 1524 | 1732 | 972 |
| R1[a] | 0.0617 | 0.0349 | 0.0489 |
| wR2[a] | 0.1721 | 0.0645 | 0.1196 |
| GOF on $F^2$ | 1.098 | 0.946 | 0.982 |
| $\Delta\rho_{min}$ and $\Delta\rho_{max}$ (e Å$^{-3}$) | 0.818 and −0.634 | 0.228 and −0.268 | 0.673 and −0.825 |

[a] $R1 = \sum||F_o| - |F_c||/\sum|F_o|$. $wR2 = \{\sum[w(F_o^2 - F_c^2)^2/\sum[w(F_o^2)^2]\}^{1/2}$.

**Table 2.** Selected Bond Lengths (Å) and Angles (deg) for **1−3**[a]

| | | | |
|---|---|---|---|
| | | **1** | |
| Mn(1)−O(2)#1 | 2.092(4) | Mn(1)−O(3)#1 | 2.180(4) |
| Mn(1)−O(2) | 2.092(4) | Mn(1)−O(4) | 2.311(3) |
| Mn(1)−O(3) | 2.180(4) | Mn(1)−O(4)#1 | 2.311(3) |
| Mn(1)#2−O(4) | 2.311(3) | | |
| O(2)#1−Mn(1)−O(2) | 180.00(10) | O(2)#1−Mn(1)−O(3) | 88.91(17) |
| O(2)−Mn(1)−O(3) | 91.09(17) | O(2)#1−Mn(1)−O(3)#1 | 91.09(17) |
| O(2)−Mn(1)−O(3)#1 | 88.91(17) | O(3)−Mn(1)−O(3)#1 | 180.00(18) |
| O(2)#1−Mn(1)−O(4) | 90.63(13) | O(2)−Mn(1)−O(4) | 89.37(13) |
| O(3)−Mn(1)−O(4) | 91.78(15) | O(3)#1−Mn(1)−O(4) | 88.22(15) |
| O(2)#1−Mn(1)−O(4)#1 | 89.37(13) | O(2)−Mn(1)−O(4)#1 | 90.63(13) |
| O(3)−Mn(1)−O(4)#1 | 88.22(15) | O(3)#1−Mn(1)−O(4)#1 | 91.78(15) |
| O(4)−Mn(1)−O(4)#1 | 180.0 | Mn(1)−O(4)−Mn(1)#2 | 124.2(2) |
| | | **2** | |
| Mn(1)−O(2)#1 | 2.078(2) | Mn(1)−O(4)#2 | 2.101(2) |
| Mn(1)−O(1) | 2.187(2) | Mn(1)−O(3) | 2.224(2) |
| Mn(1)−N(2) | 2.296(2) | Mn(1)−N(1) | 2.305(2) |
| O(2)−Mn(1)#2 | 2.078(2) | O(4)−Mn(1)#1 | 2.101(2) |
| O(2)#1−Mn(1)−O(4)#2 | 104.64(9) | O(2)#1−Mn(1)−O(1) | 89.94(8) |
| O(4)#2−Mn(1)−O(1) | 99.42(8) | O(2)#1−Mn(1)−O(3) | 98.07(8) |
| O(4)#2−Mn(1)−O(3) | 91.20(8) | O(1)−Mn(1)−O(3) | 164.68(7) |
| O(2)#1−Mn(1)−N(2) | 161.74(8) | O(4)#2−Mn(1)−N(2) | 93.61(9) |
| O(1)−Mn(1)−N(2) | 87.54(8) | O(3)−Mn(1)−N(2) | 80.75(8) |
| O(2)#1−Mn(1)−N(1) | 89.69(9) | O(4)#2−Mn(1)−N(1) | 165.67(9) |
| O(1)−Mn(1)−N(1) | 80.28(7) | O(3)−Mn(1)−N(1) | 86.70(7) |
| N(2)−Mn(1)−N(1) | 72.06(9) | | |
| | | **3** | |
| Cd(1)−O(4)#1 | 2.188(4) | Cd(1)−N(2)#2 | 2.266(4) |
| Cd(1)−O(3) | 2.314(4) | Cd(1)−O(1) | 2.329(4) |
| Cd(1)−N(1) | 2.410(5) | Cd(1)−O(2) | 2.425(4) |
| O(4)−Cd(1)#1 | 2.188(4) | N(2)−Cd(1)#3 | 2.266(4) |
| O(4)#1−Cd(1)−N(2)#2 | 114.25(18) | O(4)#1−Cd(1)−O(3) | 103.16(16) |
| N(2)#2−Cd(1)−O(3) | 87.45(15) | O(4)#1−Cd(1)−O(1) | 93.59(17) |
| N(2)#2−Cd(1)−O(1) | 151.89(16) | O(3)−Cd(1)−O(1) | 89.98(16) |
| O(4)#1−Cd(1)−N(1) | 84.15(18) | N(2)#2−Cd(1)−N(1) | 87.06(16) |
| O(3)−Cd(1)−N(1) | 172.21(14) | O(1)−Cd(1)−N(1) | 92.26(16) |
| O(4)#1−Cd(1)−O(2) | 146.86(16) | N(2)#2−Cd(1)−O(2) | 96.53(16) |
| O(3)−Cd(1)−O(2) | 89.61(15) | O(1)−Cd(1)−O(2) | 55.45(13) |
| N(1)−Cd(1)−O(2) | 85.53(15) | | |

[a] Symmetry transformations used to generate equivalent atoms: For **1**, #1 $-x, -y, -z + 2$; #2 $-x, y, -z + {}^5/_2$. For **2**, #1 $x, -y + {}^3/_2, z + {}^1/_2$; #2 $x, -y + {}^3/_2, z - {}^1/_2$. For **3**, #1 $-x + 1, -y + 2, -z + 1$; #2 $x, y + 1, z$; #3 $x, y - 1, z$.

data were corrected for underlying diamagnetism by using Pascal's constants.[10]

**Caution!** Although no problems were encountered in this work, the salt perchlorates are potentially explosive. They should be prepared in small quantities and handled with care.

**X-ray Crystallography.** Crystal data collection and refinement parameters for polymers **1−3** are given in Table 1. All measurements were made on a Rigaku RAXIS−IV imaging plate area detector with graphite monochromated Mo Kα radiation ($\lambda$ = 0.71073 Å). Red prismatic single crystals of **1−3** were selected and mounted on a glass fiber. The data were collected at a temperature of 291(2) K and corrected for Lorenz-polarization effects. A correction for secondary extinction was applied. The structures were solved by direct methods and expanded using Fourier techniques. The non-hydrogen atoms were refined anisotropically. Hydrogen atoms were included but not refined. The final cycle of full-matrix least-squares refinement was based on observed reflections and variable parameters. All calculations were performed using the SHELXL-97 crystallographic software package.[11] Selected bond lengths and bond angles are reported in Table 2.

## Results and Discussion

**Preparation of the Polymers.** Polymers **1−3** were obtained by the slow evaporation of methanol−water solutions of appropriate ligands and metal salts in neutral conditions at room temperature in the dark. In our previous paper, we provided detailed explanations of why the mixture solutions of ferrocenyl-substituted carboxylate ligands and metal ions must be placed away from light.[6c] Thus, it is without exception that the crystals suitable for X-ray crystallography of polymers **1−3** were obtained by slow evaporation of their mixture solutions in the dark.

Treatment of Mn(Ac)$_2$ and $FcC_6H_4COONa$ in a $H_2O$−$CH_3OH$ mixture solution gives one-dimensional polymer **1**, in which solvent $H_2O$ molecules bridge the Mn ions with $FcC_6H_4COO^-$ groups hanging on the two sides of the main chains. When the subsidiary ligand phen was added to the reaction system used for the preparation of **1**, the new one-dimensional polymer **2** with $FcC_6H_4COO^-$ in the main chains was obtained. To our knowledge, most of the reported ferrocene carboxylate-containing polymers have d$^{10}$ metal centers (Zn, Cd, Pb, Sn, etc.), and there are no such polymers containing Mn(II) ions. If we use Cd(II) and another kind of flexible spacer ligand, bbp, to take the place of Mn(II) and phen, respectively, the coaction of the $FcC_6H_4COO^-$ units and bbp results in the one-dimensional ladderlike framework **3**.

Polymers **1−3** are all stable in air; cannot be dissolved in common solvents such as $CH_3OH$, $CH_2Cl_2$, $C_2H_5OH$, and

---

(10) Carlin, R. L. *Magnetochemistry*; Springer: Berlin, 1986.

(11) Sheldrick, G. M. *SHELXL-97, Program for the Solution and Refinement of Crystal Structures*; University of Göttingen: Göttingen, Germany, 1997.

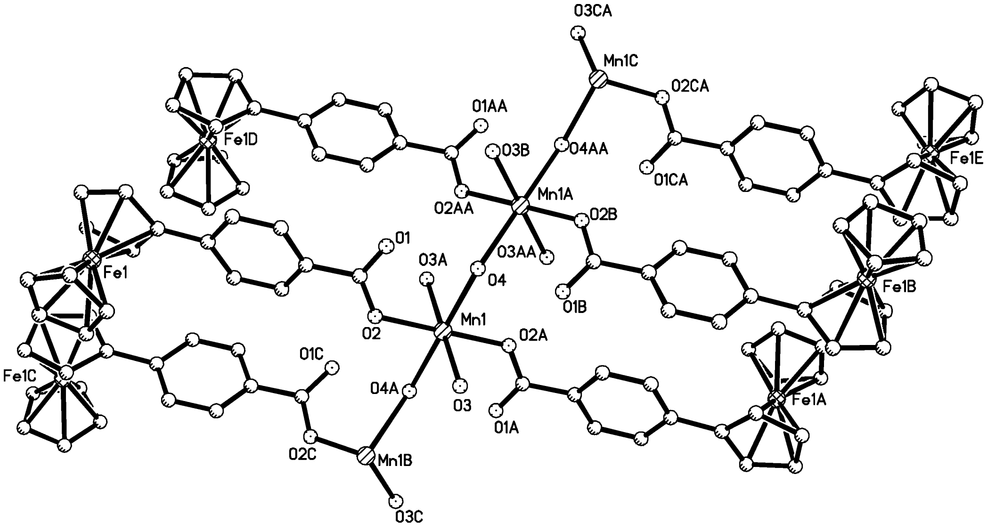

**Figure 1.** ORTEP drawing with heteroatom labeling scheme of the one-dimensional chain polymer $\{[Mn(OOCH_4C_6Fc)_2(\mu_2\text{-}OH_2)(H_2O)_2](H_2O)\}_n$ **(1)**. (Hydrogen atoms and solvent molecules are omitted for clarity.)

$CH_3CN$; and are just soluble in some highly polar solvents such as DMSO and DMF.

**Crystal Structure of $\{[Mn(OOCH_4C_6Fc)_2(\mu_2\text{-}OH_2)(H_2O)_2](H_2O)\}_n$ (1).** This molecule crystallizes in the space group *C*2/*c*. X-ray diffraction analysis reveals that, in **1**, the Mn(II) ions are bridged by $\mu_2$-$OH_2$ molecules forming one-dimensional linear chains. The ORTEP drawing with the atom labeling scheme of the one-dimensional chain polymer $\{[Mn(OOCH_4C_6Fc)_2(\mu_2\text{-}OH_2)(H_2O)_2](H_2O)\}_n$ is depicted in Figure 1, from which we can see that the coordination geometry around Mn1 is a slightly distorted octahedron. Each Mn ion coordinates with six O atoms, which come from two terminal monodentate coordinated $FcC_6H_4COO^-$ units (O2, O2A), two terminal monodentate coordinated $H_2O$ molecules (O3, O3A), and two bridging $\mu_2$-$OH_2$ molecules (O4, O4A). We can presume that the equatorial plane is composed of O2, O2A, O3, and O3A, which form a perfect plane. The O2−Mn1−O2A and O3−Mn1−O3A bond angles are both 180°, and the bond distances of Mn1−O2 and Mn1−O3 are 2.092(4) and 2.180(4) Å, respectively. The O4 and O4A atoms occupy the axial position. Because it takes part in bridging, the Mn1−O4 [2.311(3) Å] distance is longer than those of Mn1−O2 and Mn1−O3 in the equatorial position, and the axial angle O4−Mn1−O4A is 180°. Compared with some reported di-Mn(II) complexes containing ($\mu_2$-aqua)($\mu_2$-carboxylato) bridges, the $Mn{-}O_{(\mu_2-OH_2)}$ distance in **1** is a slightly longer than the corresponding Mn−O distances of $[Mn_2(\mu_2\text{-}OH_2)(\mu_2\text{-}OAc)_2(Im)_4(OAc)_2]$ (Im = imidazole) [2.246(2) Å] and $[Mn_2(\mu_2\text{-}OH_2)(\mu_2\text{-}OAc)_2(Bzim)_4(OAc)_2]$ (Bzim = benzimidazole) [2.227(2) Å],[12] and it is significantly longer than the $\mu_2$-O−Mn(III) (1.78−1.81 Å) and $\mu_2$-OH−Mn(II) (2.05−2.09 Å) distances in the literature.[13] Except for the angles mentioned above, all other angles around Mn1 are in the range of 88.22(15)−91.78(15)°, which are very close to right angles. All of the Mn atoms are connected by the bridging $H_2O$ molecules forming ···O···Mn···O···Mn··· chains with the ferrocene moieties hanging on the two sides of these chains (Figure 1). The Mn1−O4−Mn1A angle is 124.2(2)°; thus, the one-dimensional chains display a slight twist. At the same time, because of the spatial configuration and the steric effect of the ferrocene group, all of the ferrocene moieties are alternately parallel with each other along the chains. In addition, the intrachain Mn···Mn distance is 4.085 Å, which is longer than those of ($\mu_2$-aqua)-bis($\mu_2$-carboxylato) di-Mn(II) complexes, such as $[Mn_2(H_2O)(piv)_4(Me_2bpy)_2]$ [3.5950(9) Å] (piv = pivalate), $[Mn_2(H_2O)(OAc)_4(tmeda)_2]$ (tmeda = *N*,*N*,*N*′,*N*′,-tetramethylenediamine) [3.621(2) Å],[14]and a ($\mu_2$-hydroxo)bis($\mu_2$-carboxylato) complex [3.351(3) Å] in the literature[15] but shorter than that of a bis($\mu_2$-carboxylato) complex (4.298 Å) in the literature,[16] whereas the interchain Mn···Mn distance is 9.827 Å. All of the well-separated infinite chains are parallel to each other and packed along the *a* direction (Figure 2).

The $H_2O$ molecule usually participates in coordinating with metal ions in monodentate terminal fashion. Some di-Mn(II) complexes connected by a $\mu_2$-aqua bridge with the help of a $\mu_2$-carboxylato bridge have also been reported,[12,14,17] whereas $\{[Mn(OOCH_4C_6Fc)_2(\mu_2\text{-}OH_2)(H_2O)_2](H_2O)\}_n$ **1** is a rare example of Mn(II) polymers in which the Mn(II) ions are bridged only by $\mu_2$-aqua and the carboxylate groups are just hanging on the two sides of the main chain.

**Crystal Structure of $[Mn(\mu_2\text{-}OOCH_4C_6Fc)_2(phen)]_n$ (2).** The crystal structure analysis by X-ray diffraction demonstrates that **2** crystallizes in the space group *P*2(1)*c*. In **2**, the $FcC_6H_4COO^-$ units display bidentate bridging modes and

---

(12) Ye, B. H.; Mak, T.; Williams, I. D.; Li, X. Y. *Chem. Commun.* **1997**, 1813.

(13) (a) Pecoraro, V. L.; Baldwin, M. J.; Gelasso, A. *Chem. Rev.* **1994**, *94*, 807. (b) Que, L., Jr.; Trye, A. E. *Prog. Inorg. Chem.* **1990**, *38*, 97. (c) Weighardt, K. *Angew. Chem., Int. Ed. Engl.* **1989**, *28*, 1153.

(14) Yu, S.-B.; Lippard, S. J.; Shweky, I.; Bino, A. *Inorg. Chem.* **1992**, *31*, 3502.

(15) Bossek, U.; Wieghardt, K.; Nuber, B.; Weiss, J. *Inorg. Chim. Acta* **1989**, *165*, 123.

(16) Che, C. M.; Tang, W. T.; Wong, K. Y.; Wong, W. T.; Lai, T. F. *J. Chem. Res. Synop.* **1991**, 30.

(17) Caneschi, A.; Ferraro, F.; Gatteschi, D.; Melandui, M. C.; Rey, P.; Sessoli, R. *Angew. Chem., Int. Ed. Engl.* **1989**, *28*, 1365.

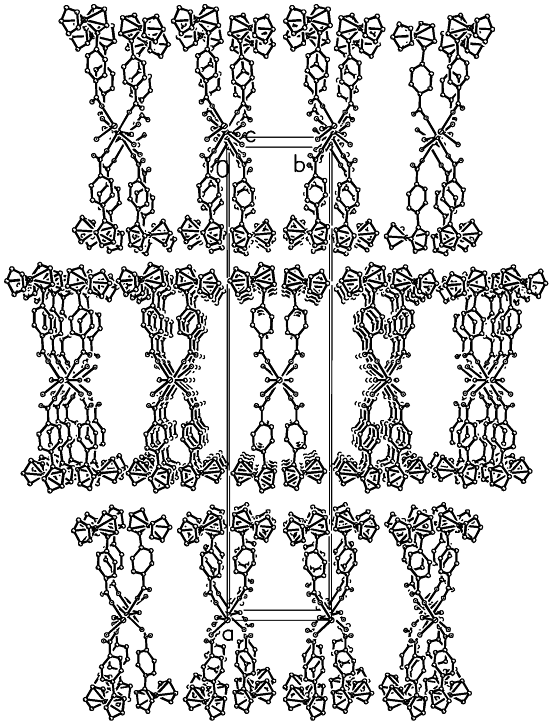

**Figure 2.** Solid-state structure of $\{[Mn(OOCH_4C_6Fc)_2(\mu_2\text{-}OH_2)(H_2O)_2](H_2O)\}_n$ **(1)**.

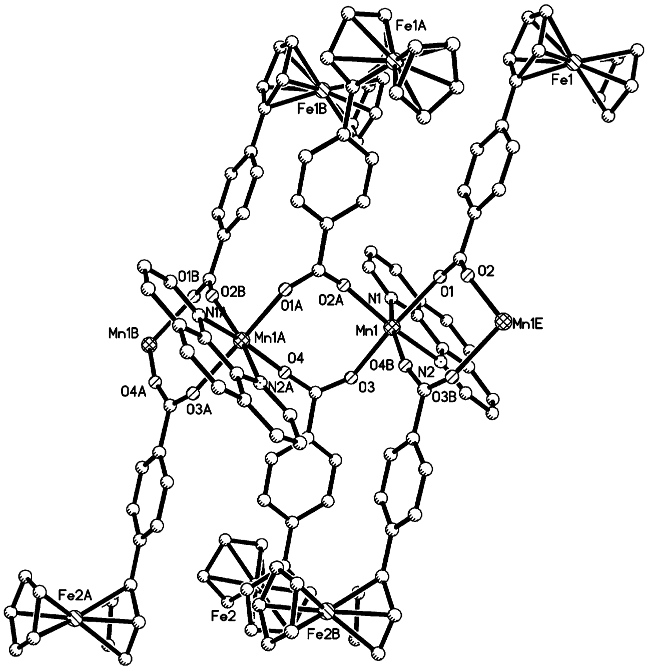

**Figure 3.** One-dimensional chain structure of $[Mn(\mu_2\text{-}OOCH_4C_6Fc)_2(phen)]_n$ **(2)** with heteroatom numbering. (Hydrogen atoms are omitted for clarity.)

connect the adjacent Mn atoms, forming a one-dimensional double-bridged chain (Figure 3). From the figure, we can see that each Mn1 atom is hexacoordinated by two N atoms (N1, N2) arising from the chelating phen and four O atoms from four different $\mu_2$-$OOCH_4C_6Fc$ units, so the Mn1 atom exhibits approximately distorted octahedral stereochemistry geometry. Mn1, N1, N2, O4B, and O2A form the basal plane (the mean deviation from the ideal plane is 0.0052 Å), the O1 and O3 atoms occupy the axial positions, and the axial angle O1−Mn1−O3 is 164.68(7)°, which is close to a flat angle. The bond lengths of Mn1−N1 and Mn1−N2 are 2.305(2) and 2.296(2) Å, respectively. This is comparable to the dimensions of an analogous one-dimensional polymer, $[Mn_2(phen)_4(\mu\text{-phth})]_n(ClO_4)_{2n}$ (phth = isophthalate),[18] in which both Mn(II) ions are bridged by two carboxylate groups coordinated in syn−syn mode, and the $Mn-N_{(phen)}$ average bond length is 2.268 Å, whereas for another analogous 1D zigzag chain polymer, $[Mn(\mu\text{-}ClCH_2COO)_2(phen)]_n$, the two $Mn-N_{(phen)}$ bond distances are equivalent (2.306 Å).[19] In **2**, the N1−Mn1−N2 angle of 72.06(9)° is far from 90°, because of the restricted geometry of phen. The distances of Mn−O range from 2.078(2) to 2.224(2) Å, which are in the range of the normal Mn−O length (~2.20 Å) in Mn(II) carboxylate complexes.[20] Between the adjacent two Mn atoms, there are two $\mu_2$-$OOCH_4C_6Fc$ units existing as double bridges that connect the two neighboring Mn atoms to an eight-membered cavity. The intrachain distance between the neighboring Mn atoms is 4.817 Å, which is slightly longer than the Mn−Mn distances of polymer **1** (4.085 Å), a bis($\mu_2$-carboxylato) complex in the literature[16] (4.298 Å), and $[Mn_2(\mu\text{-}ClCH_2COO)_2(phen)_4](ClO_4)_2\cdot 2CH_2Cl_2$ (4.613 Å)[19] and close to those of $[Mn_2(\mu\text{-phth})(phen)_4]_n(ClO_4)_{2n}$ (phth = isophthalate) (4.86 Å)[18] and $[Mn\cdot PDB\cdot H_2O]_n$ ($H_2PDB$ = pyridine-3,4-dicarboxylic acid) (ca. 4.8 Å),[21] but it is much shorter than those of $\{[Mn(bic)Cl]_2\cdot 2(H_2O)\}_n$ (bic = bicinate) (4.978 Å),[22] $[Mn(C_5H_6NO_3)_2]_\infty$ (5.086 Å),[23] $[Mn(MPCA)_2(H_2O)]_n$ (MPCA = 2-methyl-4-choro phenoxyacetic acid) (5.4 Å),[24] $[Mn(pzca)_2]_n$ (pzca = 2-pyrazinecarboxylate) (5.654 Å),[25] and some polynuclear complexes, such as $[\{Mn(bipy)_2(H_2O)\}_2\{(CH_3)_3NCH_2CO_2\}](ClO_4)_4\cdot 2H_2O$ (5.598 Å),[26] whereas for polymer **2**, the shortest interchain distance between two Mn atoms is 9.085 Å. In contrast with polymer **1**, the Mn(II) ions in **2** are connected by these $\mu_2$-$OOCH_4C_6Fc$ units, forming a one-dimensional double-bridged chain polymer. In the solid-state structure of **2** (Figure 4), all of the Mn(II) ions are bridged by the $\mu_2$-$OOCH_4C_6Fc$ units forming pseudo-channels along the *c* direction.

The phen rings are coplanar, and they are parallel to each other along the 1D chains. The shortest distance between two parallel phen rings within the chain is 8.223 Å, and the dihedral angle between adjacent phen planes is 4.3°, which

---

(18) Tan, X. S.; Sun, J.; Xiang, D. F.; Tang, W. X. *Inorg. Chim. Acta* **1997**, *255*, 157.

(19) Fernández, G.; Corbella, M.; Mahía, J.; Maestro, M. A. *Eur. J. Inorg. Chem.* **2002**, 2502.

(20) Halcrow, M. A.; Streib, W. E.; Folting, K.; Christou, G. *Acta Cryst.* **1995**, *C51*, 1263.

(21) Chen, W.; Yue, Q.; Chen, C.; Yuan, H. M.; Xu, W.; Chen, J. S.; Wang, S. N. *J. Chem. Soc., Dalton Trans.* **2003**, 28.

(22) Sun, Z. M.; Gantzel, P. K.; Hendrickson, D. N. *Polyhedron* **1997**, *16*, 3267.

(23) Gutschke, S. O. H.; Price, D. J.; Powell, A. K.; Wood, P. T. *Inorg. Chem.* **2000**, *39*, 3705.

(24) Tangoulis, V.; Psomas, G.; Dendrinou-Samara, C.; Raptopoulou, C. P.; Terzis, A.; Kessissoglou, D. P. *Inorg. Chem.* **1996**, *35*, 7655.

(25) Liang, Y. C.; Hong, M. C.; Liu, J. C.; Cao, R. *Inorg. Chim. Acta* **2002**, *328*, 152.

(26) Chen, X. M.; Tong, Y. X.; Xu, Z. T.; Mak, T. C. W. *J. Chem. Soc., Dalton Trans.* **1995**, 4001.

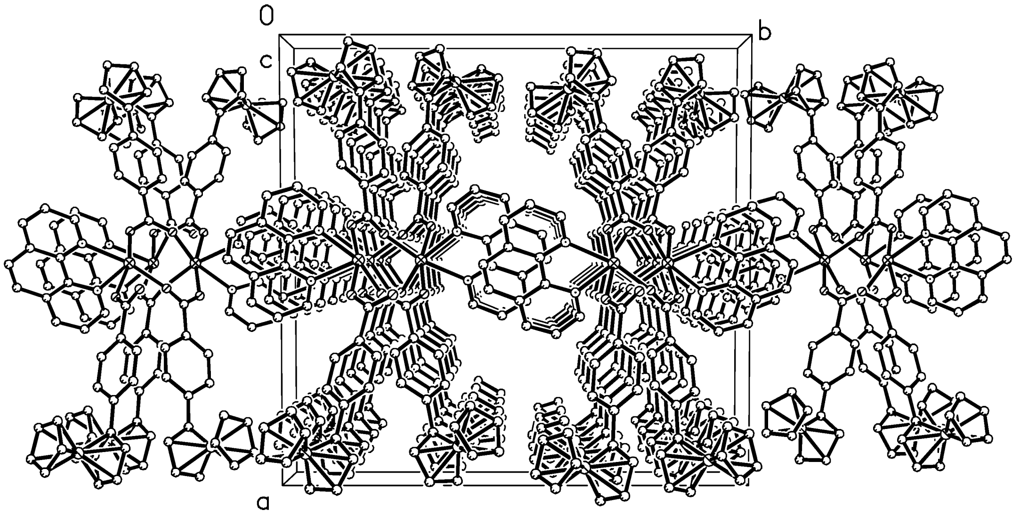

**Figure 4.** Solid-state structure of {[Mn($\mu_2$-OOCH$_4$C$_6$Fc)$_2$(phen)]$_n$ **(2)** showing the one-dimensional chain extended along the *c* direction.

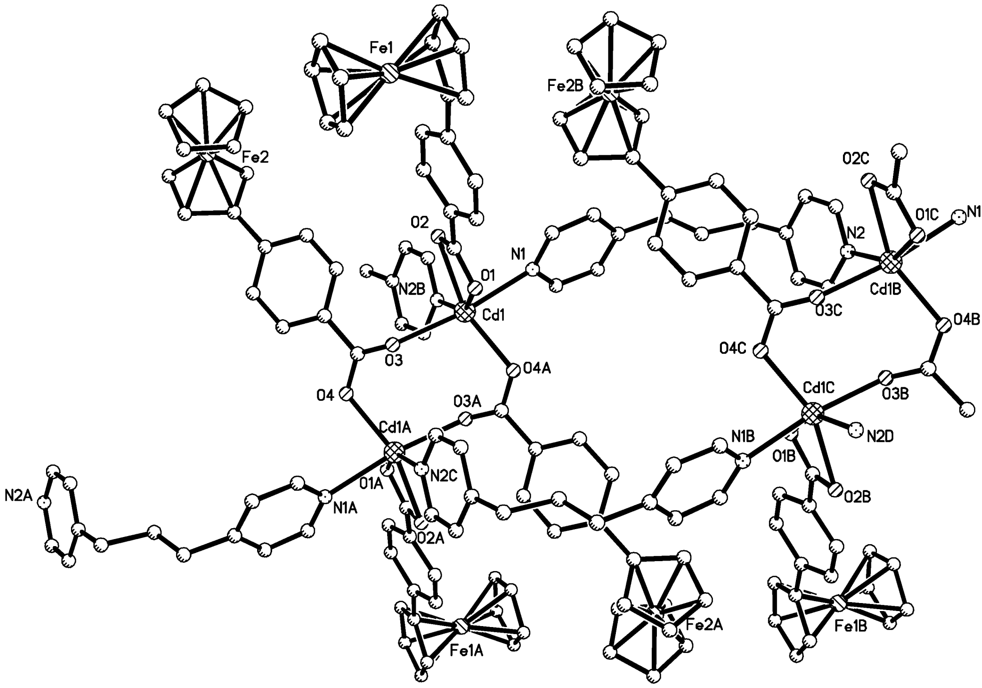

**Figure 5.** Perspective view of the one-dimensional chain structure of {[Cd($\mu_2$-OOCH$_4$C$_6$Fc) ($\eta^2$-OOCH$_4$C$_6$Fc)(bbp)](CH$_3$OH)}$_n$ **(3)** (Hydrogen atoms are omitted for clarity.)

is out of the limit of the common range for $\pi\cdots\pi$ interactions between two aryl rings.[27] Thus, no obvious intermolecular $\pi\cdots\pi$ interactions are found between these phen rings in contrast to the known Mn−phen−dicarboxylato complexes reported previously.[28]

**Crystal Structure of {[Cd($\mu_2$-OOCH$_4$C$_6$Fc)($\eta^2$-OOCH$_4$C$_6$Fc)(bbp)](CH$_3$OH)}$_n$ (3).** The crystal structure of **3** consists of an infinite one-dimensional ladderlike framework in which the neighboring Cd(II) ions are linked by the coaction of the FcC$_6$H$_4$COO$^-$ and the flexible bridging ligand bbp (Figure 5).

The Cd1 atom exhibits a hexacoordinate stoichiometry; the coordination geometry around the Cd atoms is illustrated in Figure 5. Each Cd atom bonds to two O atoms from the chelating FcC$_6$H$_4$COO$^-$ unit, two O atoms from two bridging $\mu_2$-OOCH$_4$C$_6$Fc units, and two N atoms from bbp. The Cd−O distances are in the range of 2.188(4)−2.425(4) Å, and the Cd1−N1 and Cd1−N2B distances are 2.410(5) and 2.266(4) Å, respectively. The N1−Cd1−N2B angle is 87.06(16)°, so the two pyridine rings connecting to one Cd atom are nearly perpendicular. The FcC$_6$H$_4$COO$^-$ units have two kinds of coordination modes: one is that each FcC$_6$H$_4$COO$^-$ unit coordinates with one Cd atom as a chelating bidentate ligand, and the other is that each FcC$_6$H$_4$COO$^-$

---

(27) (a) Guo, D.; Pang, K.-L.; Duan, C.-Y.; He, C.; Meng, Q.-J. *Inorg. Chem.* **2002**, *41*, 5978. (b) Shriver, D. F.; Arkins, P.; Langford, C. H. *Inorganic Chemistry*, 2nd ed.; W. H. Freeman and Company: New York, 1997.

(28) (a) Zheng, Y.-Q.; Lin, J.-L.; Sun, J. In *Abstracts of the Ninth International Conference on Inorganic Ring Systems*; Saarbrücken, Germany, 2000; pp 1−61. (b) Zheng, Y.-Q.; Sun, J.; Lin, J.-L. *Anorg. Allg. Chem.* **2001**, *627*, 1059. (c) Wei, D.-Y.; Kong, Z.-P.; Zheng, Y.-Q. *Polyhedron* **2002**, *21*, 1621. (d) Zheng, Y.-Q.; Kong, Z.-P. *J. Chem. Crystallogr.* **2002**, *32*, 119.

unit bridges two adjacent Cd atoms as a $\mu_2$-bidentate bridging ligand. The neighboring two Cd(II) ions are connected by $\mu_2$-$OOCH_4C_6Fc$ groups forming a binuclear unit, within which the Cd⋯Cd distance is 4.541 Å, and all of the binuclear groups are joined together by the flexible bbp. Compared with the reported Cd(II)-bbp polymer $[Cd(dca)_2(bbp)]_\infty$ (dca = dicynamido anion),[29] the arc-shaped bbp in **3** adopts a gauche conformation with a much larger pyridyl-to-pyridyl dihedral angle (91.6°) and slightly shorter N-to-N distance (9.206 Å within the bbp), the corresponding pyridyl-to-pyridyl dihedral angle and N-to-N distance of $[Cd(dca)_2(bbp)]_\infty$ are 79.7° and 9.41 Å, respectively. The Cd-to-Cd distances spanned by the double bbp bridges is 12.354 Å, which is slightly shorter than the corresponding Cd-to-Cd distance of $[Cd(dca)_2(bbp)]_\infty$ (12.72 Å). Also, the one-dimensional ladderlike chains extended along the [010] direction. This is comparable to the reported ferrocenecarboxylate Zn(II) polymer $[Zn(FcCOO)(\eta^2\text{-}FcCOO)(bbp)]_n$,[6d] in which the metal ions are connected by the bbp ligands leading to an infinite −Zn−bbp−Zn−bbp− zigzag chain.

**Redox Properties.** We determined the molecular weights of polymers **1**−**3** in DMF solution. The results show that the number-average molecular weights ($M_n$) are 7.262 × $10^4$ for polymer **1**, 3.592 × $10^4$ for polymer **2**, and 1.998 × $10^4$ for polymer **3**. The weight-average molecular weights ($M_w$) are 1.508 × $10^5$, 2.454 × $10^5$, and 2.738 × $10^4$ for polymers **1**−**3**, respectively. Thus, we can confirm that polymers **1**−**3** are intact in DMF solution.

The electrochemical behaviors of **1**−**3** and free sodium *p*-ferrocenylbenzoate were studied by cyclic voltammograms at a platinum electron in DMF (see Supporting Information). The observed redox peaks correspond to the redox processes of the ferrocene moieties, all of which undergo a quasireversible one-electron oxidation process based on the ferrocene unit. The half-wave potentials ($E_{1/2}$) of **1**−**3** and the corresponding sodium *p*-ferrocenylbenzoate in DMF solution are 0.546, 0.543, 0.532, and 0.528 V (vs SCE), respectively, and their $\Delta E_p$ values are 127, 116, 149, and 159 mV, respectively. Compared with the free sodium *p*-ferrocenylbenzoate, the coordination of the metal ions to the *p*-ferrocenylbenzoate makes the redox properties of the polymers markedly different because the ferrocene redox couples ($E_{1/2}$) are all shifted to higher potentials. This situation is consistent with the previous results of transition metal−ferrocenyl system.[6b,30] The difference in the electrochemical behavior is due to the presence of the conjugated $\pi$-electron systems between the two metals that allow communication[31] and the electron-withdrawing nature of the coordinated metal centers that make the ferrocene unit harder to oxidize.[32]

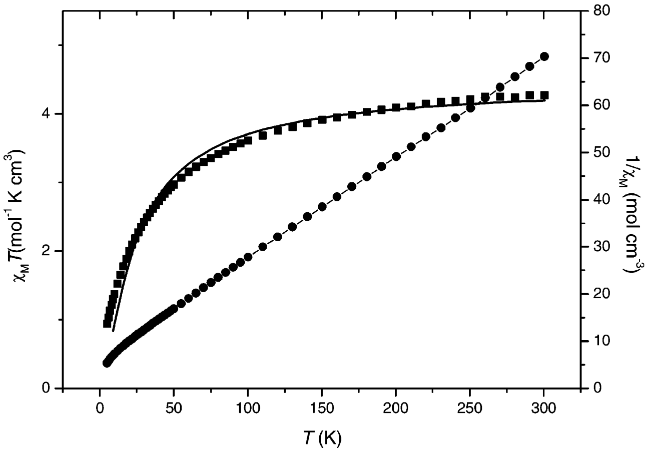

**Figure 6.** Temperature dependence of $\chi_M T$ of **1** investigated over the temperature range 300−5 K at 500 G and the experimental data plotted as the thermal variation of the reciprocal susceptibility $\chi_M^{-1}$.

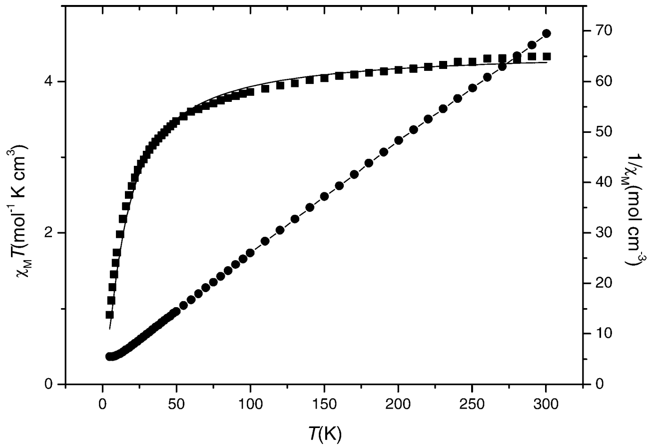

**Figure 7.** Temperature dependence of $\chi_M T$ of **2** investigated over the temperature range 300−5 K at 500 G and the experimental data plotted as the thermal variation of the reciprocal susceptibility $\chi_M^{-1}$.

**Magnetic Properties.** The magnetic susceptibilities of **1** and **2** were measured in the 5−300 K temperature range and are shown as $\chi_M^{-1}$ and $\chi_M T$ versus $T$ plots in Figures 6 and 7.

At room temperature, both $\chi_M T$ values (4.28 cm$^3$ K mol$^{-1}$ for **1** and 4.32 cm$^3$ K mol$^{-1}$ for **2**) are close to the expected value for an uncoupled Mn(II) ion ($g = 2.0$, $\chi_M T = 4.38$ cm$^3$ K mol$^{-1}$). As the temperature decreases, $\chi_M T$ decreases continuously and reaches 0.938 and 0.914 cm$^3$ K mol$^{-1}$ at 5 K for **1** and **2**, respectively. This magnetic behavior indicates the occurrence of an antiferromagnetic interaction between the Mn(II) ions for the two polymers. The close approximation between the experimental moments of **1** (5.85$\mu_B$) and **2** (5.88$\mu_B$) and the theoretical spin-only value for $S = {}^5/_2$ ($\mu_{eff} = 5.92\mu_B$) suggests that these complexes contain largely isolated spins. A plot of $\chi_M^{-1}$ versus $T$ gives two straight lines (Figures 6 and 7) that can be fitted to the Curie−Weiss

---

(29) Gao, E. Q.; Bai, S. Q.; Wang, Z. M.; Yan, C. H. *J. Chem. Soc., Dalton Trans.* **2003**, 1759.

(30) (a) Horikoshi, R.; Mochida, T.; Moriyama, H. *Inorg. Chem.* **2002**, *41*, 3017. (b) Barranco, E. M.; Crespo, O.; Gimeno, M. C.; Jones, P. G.; Laguna, A.; Villacampa, M. D. *J. Organomet. Chem.* **1999**, *592*, 258. (c) Duan, C. Y.; Tian, Y. P.; Liu, Z. H.; You, X. Z.; Mak, T. C. W. *J. Organomet. Chem.* **1998**, *570*, 155. (d) Sun, S. S.; Anspach, J. A.; Lees, A. J. *Inorg. Chem.* **2002**, *41*, 1862. (e) Ion, A.; Buda, M.; Moutet, J. C.; Saint-Aman, E.; Royal, G.; Gautier-Luneau, I.; Bonin, M.; Ziessel, R. *Eur. J. Inorg. Chem.* **2002**, 1357.

(31) (a) Long, N. J. *Metallocenes*; Blackwell: Oxford, U.K., 1998. (b) Beer, P. D.; Blackburn, C.; McAleer, J. F.; Sikanyika, H. *Inorg. Chem.* **1990**, *29*, 378. (c) Carr, J. D.; Coles, S. J.; Hursthouse, M. B.; Light, M. E.; Munro, E. L.; Tucker, J. H. R.; Westwood, J. *Organometallics.* **2000**, *19*, 3312.

(32) Barranco, E. M.; Crespo, O.; Gimeno, M. C.; Jones, P. G.; Laguna, A.; Sarroca, C. *J. Chem. Soc., Dalton Trans.* **2001**, 2523.

law $\chi_M = C/(T - \theta)$ with $C = 4.632$ and $\theta = -26.54$ K for **1** and $C = 4.524$ and $\theta = -15.97$ K for **2**. The negative values of $\theta$ confirm the antiferromagnetic exchange interaction between the Mn(II) ions for **1** and **2**.

The Mn(II) ion has a large quantum spin number ($S = {}^5/_2$) and a small spin anisotropy because of negligible spin−orbit coupling, so the data can be analyzed assuming a classical isotropic Heisenberg pairwise interaction between Mn(II) ions in a linear chain. The spin Hamiltonian is given in eq 1, from which many sophisticated models have derived. The most appropriate is the result of Fisher chain model (eq 2),[33] which is valid for large values of $S$.

$$H = -2J\sum_{i=1}^{n} S_i S_{i-1} \tag{1}$$

$$\chi = \frac{Ng^2\beta^2 S(S+1)}{3kT} \times \frac{(1+u)}{(1-u)} \tag{2}$$

where

$$u = \coth\frac{|J|S(S+1)}{kT} - \frac{kT}{|J|S(S+1)}$$

Using this model we derive the best least-squares fits of the experimental data of $J = -5.20$ cm$^{-1}$ and $g = 2.02$ for **1** and $J = -3.25$ cm$^{-1}$ and $g = 2.01$ for **2**, with agreement factors of $R = 3.5 \times 10^{-3}$ and $8.7 \times 10^{-4}$ for **1** and **2**, respectively. The antiferromagnetic exchange interactions between Mn(II) ions in polymer **1** is stronger than those in **2**.

The observed magnetism in polymers **1** and **2** can be explained by structural considerations. It is worth noting that the magnetic exchange pathways between Mn(II) ions in **1** and **2** are quiet different. The magnetic exchange in **1** is supported by the $\mu_2$-aqua bridge forming the Mn···O···Mn pathway, whereas in **2**, it is conducted through bridging carboxylate groups forming two identical Mn···O···C···O···Mn pathways. In most cases, the magnetic exchange between two metals is produced through several pathways, but the shortest superexchange pathways usually mediate the strongest spin−spin interactions.[23]

Recently, many carboxylate-bridged dinuclear Mn(II),[12,14,17] polynuclear Mn(II),[34] and 1D Mn(II) polymers[35,36] have been prepared, and their magnetic properties have been extensively explored. The magnetic exchange parameters $J$ of **1**, **2**, and some known di-Mn(II) complexes and one-dimensional polymers are listed in Table 3. From the table, we can see that the exchange interaction between Mn(II) ions is mainly antiferromagnetic and the $J$ values for **1** (−5.20 cm$^{-1}$) and **2** (−3.25 cm$^{-1}$) are larger than those of the di-Mn(II) complexes and one-dimensional Mn(II) polymers. A few examples such as $[Mn_2(F_5C_2COO)_4(H_2O)_3L_2]$[17] and $[Mn_2(\mu\text{-phth})(phen)_4]_n(ClO_4)_{2n}$ display weak ferromagnetic exchange interactions.[18]

**Table 3.** Comparison of Magnetic Exchange Parameter [$J$ (cm$^{-1}$)] for Some Reported di-Mn(II) Complexes Containing $\mu_2$-Aqua and $\mu_2$-Carboxylato Bridges and One-Dimensional Mn(II) Carboxylic Polymers

| formula[a] | $J$ (cm$^{-1}$) | ref |
|---|---|---|
| di-Mn(II) Complexes | | |
| $[Mn_2(H_2O)(piv)_4(Me_2bpy)_2]$ | −2.73(2) | 14 |
| $[Mn_2(H_2O)(OAc)_4(tmeda)_2]$ | −2.952(7) | 14 |
| $[Mn_2(F_5C_2COO)_4(H_2O)_3L_2]$ | 3.3(0.2) | 17 |
| $[Mn_2(\mu_2{-}OH_2)(\mu_2{-}OAc)_2(Im)_4(OAc)_2]$ | −1.26 | 12 |
| $[Mn_2(\mu_2{-}OH_2)(\mu_2{-}OAc)_2(Bzim)_4(OAc)_2]$ | * | 12 |
| 1D Mn(II) Polymers | | |
| $[Mn(C_5H_6NO_3)_2]_\infty$ | −0.376(1) | 23 |
| $\{[Mn(bic)Cl]_2{\cdot}2(H_2O)\}_n$ | −0.30 | 22 |
| $\{[Mn(bic)(H_2O){\cdot}2Br{\cdot}2H_2O]_n$ | −1.42(2) | 34 |
| $[Mn{\cdot}PDB{\cdot}H_2O]_n$ | * | 21 |
| $[Mn_2(\mu\text{-phth})(phen)_4]_n(ClO_4)_{2n}$ | 3.23 | 18 |
| $[Mn(\mu\text{-}ClCH_2COO)_2(phen)]_n$ | −0.89 | 19 |
| $[Mn(\mu{-}3\text{-}ClC_6H_4COO)_2(bpy)]_n$ | −1.72 | 37 |
| $\{[Mn(OOCH_4C_6Fc)_2(\mu_2{-}OH_2)(H_2O)_2](H_2O)\}_n$ | −5.20 | this work |
| $[Mn(\mu_2{-}OOCH_4C_6Fc)_2(phen)]_n$ | −3.25 | this work |

[a] Abbreviations: piv = pivalate, tmeda = *N,N,N′,N′*-tetramethylenediamine, L = 2-ethyl-4,4,5,5-tetramethyl-3-oxo-4,5-dihydro-1H-imadazolyl-1-oxyl, Im = imidazole, Bzim = benzimidazole, bic = bicinate, $H_2PDB$ = pyridine-3,4-dicarboxylic acid, phth = isophthalate, phen = phenanthroline. * No $J$ value in the reported articles.

**Acknowledgment.** The authors thank the National Natural Science Foundation of China (Nos. 20001006 and 20371042), the Excellent Young Teachers Program in Higher Education Institute, and Henan Province for financial support.

**Supporting Information Available:** Crystallographic data in CIF format. Thermogravimetric analysis procedure and results for polymers **1**−**3** and cyclic voltammograms for polymers **1**−**3** and free sodium *p*-ferrocenylbenzoate. This material is available free of charge via the Internet at http://pubs.acs.org.

IC049728X

---

(33) Fisher, M. E. *Am. J. Phys.* **1964**, *32*, 343.

(34) (a) Vincent, J. B.; Christmas, C.; Chang, H. R.; Li, Q.; Boyd, P. D. W.; Huffman, J. C.; Hendrickson, D. N.; Christou, G. *J. Am. Chem. Soc.* **1989**, *111*, 2086. (b) Wang, S.; Huffman, J. C.; Folting, K.; Streib, W. E.; Lobkovsky, E. B.; Christou, G. *Angew Chem., Int. Ed. Engl.* **1991**, *30*, 1672.

(35) (a) Wagner, G. R.; Friedberg, S. A. *Phys. Lett.* **1964**, *9*, 11. (b) Dingel, R.; Lines, M. E.; Holts, S. L. *Phys. Rev.* **1969**, *187*, 643. (c) Weng, W.; Bartik, T.; Gladysz, J. A. *Angew Chem., Int. Ed. Engl.* **1994**, *33*, 2199. (d) Cicha, W. V.; Hayes, J. S.; Oliver, K. W.; Rettig, S. J.; Thompson, R. C.; Trotter, J. *Can. J. Chem.* **1985**, *63*, 1055. (e) Du, J.-L.; Rettig, S. J.; Thompson, R. C.; Trotter, J. *Can. J. Chem.* **1992**, *70*, 732. (f) Bino, P. B. A.; Du, J.-L.; Lo, L. S.-M.; Thompson, R. C. *Inorg. Chim. Acta* **1990**, *170*, 45.

(36) (a) Borras-Alamenar, J. J.; Burriel, R.; Coronado, E.; Gatteschi, D.; Gomez-Garcia, C. J.; Zanchini, C. *Inorg. Chem.* **1991**, *30*, 947. (b) Borras-Alamenar, J. J.; Coronado, E.; Gomez-Garcia, C. J.; Gatteschi, D.; Zanchini, C. *J. Appl. Phys.* **1990**, *67*, 6006. (c) Biagini-Cingi, M.; Manotti-Lanfredi, A. M.; Ugozzoli, F.; Haasnoot, J. G.; Reedijk, J. *Gazz. Chim. Ital.* **1994**, *124*, 509.

(37) Albela, B.; Corbella, M.; Ribas, J.; Castro, I.; Sletten, J.; Stoeckli-Evans, H. *Inorg. Chem.* **1998**, *37*, 788.